Published in final edited form as:

Arterioscler Thromb Vasc Biol. 2019 July ; 39(7): 1419–1431. doi:10.1161/ATVBAHA.118.312346.

Peroxynitrite-mediated SIRT1 Inactivation Contributes to Nicotine-induced Arterial Stiffness in Mice

Ye Ding, **Yi Han**, **Qiulun Lu**, **Junqing An**, **Huaiping Zhu**, **Zhonglin Xie**, **Ping Song**, and **Ming-Hui Zou**

Center for Molecular and Translational Medicine, Georgia State University, 157 Decatur Street SE, Atlanta, GA 30303

Abstract

Objective——Inhibition of Sirtuin-1 (SIRT1), a nicotinamide adenine dinucleotide-dependent protein deacetylase, is linked to cigarette smoking-induced arterial stiffness, but the underlying mechanisms remain largely unknown. The aim of the present study was to determine the effects and mechanisms of nicotine, a major component of cigarette smoke, on SIRT1 activity and arterial stiffness.

Approach and Results——Arterial stiffness, peroxynitrite ($ONOO^-$) formation, SIRT1 expression and activity were monitored in mouse aortas of eight-week-old C57BL/6 mice (wild-type) or *Sirt1*-overexpressing ($Sirt1^{Super}$) mice with or without nicotine for 4 weeks. In aortas of wild-type mice, nicotine reduced SIRT1 protein and activity by ≈ 50% without affecting its mRNA levels. In those from $Sirt1^{Super}$ mice, nicotine also markedly reduced SIRT1 protein and activity to the levels that were comparable to those in wild-type mice. Nicotine infusion significantly induced collagen I, fibronectin, and arterial stiffness in wild-type but not $Sirt1^{Super}$ mice. Nicotine increased the levels of inducible nitric oxide synthase and the co-staining of SIRT1 and 3-nitrotyrosine, a footprint of $ONOO^-$ in aortas. Tempol, which ablated $ONOO^-$ by scavenging superoxide anion, reduced the effects of nicotine on SIRT1 and collagen. Mutation of zinc-binding cysteine 395 or 398 in SIRT1 into serine (C395S) or (C398S) abolished SIRT1 activity. Furthermore, $ONOO^-$ dose-dependently inhibited the enzyme and increased zinc release in recombinant SIRT1. Finally, we found SIRT1 inactivation by $ONOO^-$ activated the Yes-associated protein (YAP) resulting in abnormal extracellular matrix remodeling.

Conclusions——Nicotine induces $ONOO^-$, which selectively inhibits SIRT1 resulting in a YAP-mediated extracellular matrix remodeling.

Graphical Abstract

To whom correspondence should be addressed: Ping Song, Ph.D. or Ye Ding, Ph.D., Center for Molecular and Translational Medicine, Georgia State University, 157 Decatur Street SE, Atlanta, GA, 30303, USA, Phone: 404-413-6636, yding5@gsu.edu.
Ye Ding and Yi Han contributed equally to this work.

Disclosures
None.

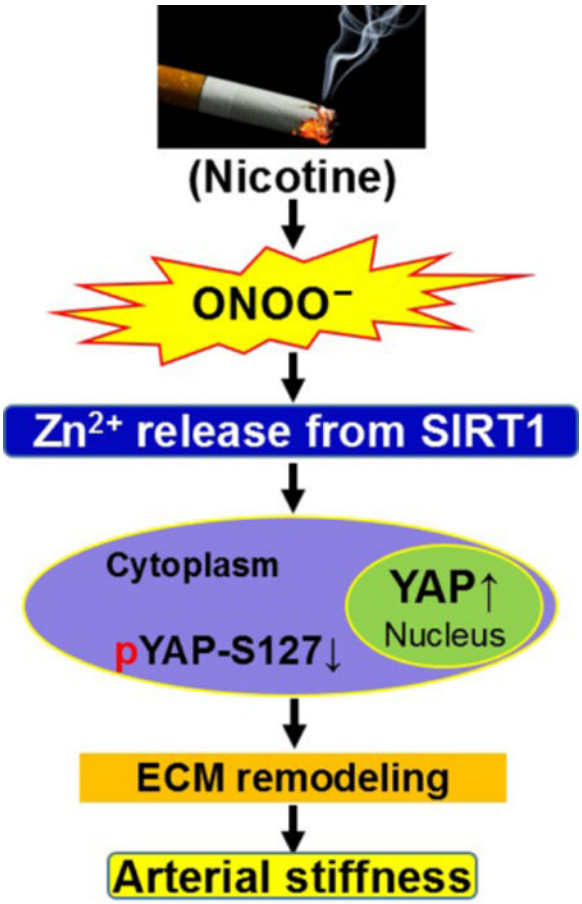

Keywords

arterial stiffness; nicotine; sirtuin-1; peroxynitrite; extracellular matrix

Introduction

Cardiovascular disease remains the leading cause of death worldwide, claiming more death each year than all cancer types combined, claiming nearly 18 million death in 2015 alone (http://www.who.int/mediacentre/factsheets/fs317/en/). Arterial stiffness, characterized by vascular wall remodeling and progressive loss of elastic properties of central and conduit arteries, is a major and independent risk factor for cardiovascular events[1] and an independent predictor of hypertension, coronary artery disease, heart attack, and heart failure.[2, 3] Arterial stiffness is also associated with stroke, cognitive impairment, and kidney failure,[4, 5] additional high-impact killers that cost patients, families, healthcare providers, and workplaces billions each year. Clearly, identifying novel treatment approaches for enhanced arterial stiffness has the potential to significantly impact the quality of life for millions and significantly reduce the economic burden of associated disease-but new treatment approaches are dependent on fully understanding the biological mechanisms behind arterial stiffness.

There are several risk factors for arterial stiffness, including aging,[6] type 2 diabetes,[7, 8] obesity,[9] and serum uric acid;[10] however, smoking is one of the most significant (and easily preventable) contributors to arterial stiffness. Smoking just one cigarette acutely and significantly increases both brachial and aortic stiffness in healthy young chronic smokers and nonsmokers; aortic systolic blood pressure is also increased in young chronic smokers.[11] Cigarette smoking also acutely increases arterial stiffness and blood pressure in hypertensive male smokers.[12] Conversely, smoking cessation decreases arterial stiffening, with profound linear relationship between how long a person has stopped smoking and the decrease in arterial stiffness.[13] Importantly, in healthy young non-smokers, acute administration of nicotine, a key component of cigarettes,[14] increases carotid-femoral pulse-wave velocity (PWV),[15] the gold-standard for assessing arterial wall stiffness.[11, 13] Additionally, despite the widespread belief that electronic cigarettes (E-cigarettes) are not associated with the same detrimental effects as traditional cigarettes, E-cigarettes have been reported to increase aortic stiffness and blood pressure in young smokers.[16]

The mechanism behind nicotine-induced arterial stiffness remains unknown. It is likely that either vascular smooth muscle cells (VSMC)[17, 18] or endothelial cells (EC)[1] play a critical role. Emerging data demonstrate that sirtuin-1 (SIRT1), an oxidized nicotinamide adenine dinucleotide (NAD^+)-dependent class III protein deacetylase, plays an important role in vascular remodeling, including neointima formation after vascular damage[19] and abdominal aortic aneurysm.[20] It has also been reported that SIRT1 activation protects against obesity-induced arterial stiffness by stimulating anti-inflammatory and antioxidant pathways in the aorta.[21] Furthermore, we had previously demonstrated that arterial PWV is significantly increased in VSMC-specific *Sirt1*-knockout mice in response to angiotensin II treatment.[20] Therefore, it seems likely that SIRT1 plays an important role in arterial stiffness.

Pathologically, increased arterial stiffness is attributed to extracellular matrix (ECM) remodeling, including induction of abnormal collagen and reduction in normal elastin, and elevated inflammation, oxidative stress, and endothelial dysfunction;[22] however, it remains unknown whether nicotine or SIRT1 affect ECM remodeling and the consequent arterial stiffness. Here we demonstrate that genetically increased *Sirt1* attenuates nicotine-induced arterial stiffness in murine aortas. We further determine that nicotine increases peroxynitrite ($ONOO^-$), which causes zinc release from SIRT1, deactivating the protein. SIRT1 deactivation then potentiates Yes-associated protein (YAP) activation and subsequent ECM remodeling, providing a novel mechanism for nicotine-induced arterial stiffness.

Materials and Methods

The authors declare that all supporting data are available within the article and in the online-only Data Supplement.

Materials and Reagents

The information for specific primary antibodies was presented in online Major Resources Tables. Nicotine (n3876–25 mL), SIRT1 Assay Kit (CS1040), Elastic Stain Kit (HT25A), Masson Trichrome Stain Kit (HT15), and Tempol (4-hydroxy-2,2,6,6-tetramethylpiperdine-1-oxyl, Cat. # 8401300100) were all purchased from Sigma-Aldrich

(St. Louis, Missouri). Hydroxyproline Colorimetric Assay Kit (Cat. #K555) was from BioVision (Milpitas, CA).

Animals

Wild-type (WT) C57 BL/6J and *Sirt1*-overexpressing (*Sirt1*^{Super}) mice[23] (Stock No: 024510) were obtained from The Jackson Laboratory (Bar Harbor, Maine). Both male and female mice were housed in temperature-controlled cages under a 12-hour light-dark cycle and given free access to water and a normal laboratory diet. All experimental procedures involving animals were approved by the Institutional Animal Care and Use Committee at Georgia State University. At 8 weeks of age, WT and *Sirt1*^{Super} mice were infused with nicotine (5 mg/kg/day) or physiological saline (0.9% sodium chloride) for four weeks using Alzet osmotic pumps (Model 2006, DURECT Corporation, Cupertino, CA) as described previously (There are 4 groups, n=10 in each group including 5 male and 5 female mice).[24] Saline- or nicotine-infused WT mice were treated with or without Tempol (30 mmol/L) in drinking water[25] for four weeks (There are 4 groups, n=10 in each group including 5 male and 5 female mice).

Human aortic smooth muscle cell culture, nicotine treatment and nuclear isolation

Human aortic smooth muscle cells (hASMCs) were grown in M231 medium to 70–80% confluence. The sex of the hASMCs is unknown. Cells were used between passages 3 and 8, and grown to 70–80% confluence before being treated with different reagents. 0.5–1 μM nicotine was used to treat hASMCs for 24h in this study. hASMCs were pretreated with10 μM Tempol for 1 hour followed by 0.5 μM nicotine treatment for 24h. Nuclei were extracted from hASMCs and murine aortas using the NE-PER™ Nuclear and Cytoplasmic Extraction Reagents (Thermo Fisher Scientific, Waltham, Massachusetts) per manufacturer's instructions.

Morphological and immunohistochemical analyses of mouse aortas

To assess murine aortas morphologically and immunohistologically following nicotine infusion and euthanasia, aortas were perfused with saline and fixed with 10% formalin in PBS for 5 minutes. Whole aortas were then harvested, fixed, and embedded in paraffin, and 5-μm cross-sections were prepared.[26] Paraffin-embedded sections were stained with hematoxylin and eosin (IW-3100, IHC World, Woodstock, Maryland) for basic morphological determination. Van Gieson Solution Acid Fuchsin (HT25A, Sigma-Aldrich, St. Louis, Missouri) were used for elastic fiber staining in aortas. Trichrome Staining (HT15, Sigma-Aldrich, St. Louis, Missouri) was performed for measuring collagen and IHC staining was carried out for detecting several protein expression (collagen I, fibronectin, SIRT1, 3-NT, iNOS, YAP, and pYAP) using the EnVision® + Dual Link System-HRP (DAB +) (K4065, Dako, Glostrup Municipality, Denmark). Negative controls were set by omitting primary antibodies. Collagen deposition areas were calculated using ImageJ (NIH, Bethesda, Maryland). To quantify elastin fragmentation, we counted the number of observed elastin breaks in the aorta. To estimate the degree of positive staining for each individual marker, a semi-quantitative analysis of tissue immunoreactivity was done by 4 observers blinded to the identity of the samples using an arbitrary grading as follows: score 1: 0–25% positive

staining in media; score 2: 26–50% positive staining in media; score 3: 51–75% positive staining in media; score 4: 76–100% positive staining in media.

Artery assay of motion (M)-mode, circumferential cyclic strain, and pulse wave velocity

Vascular ultrasound was performed using a Vevo 3100 Imaging System (FUJIFILM VisualSonics, Toronto, Canada). Prior to ultrasound, each mouse was anesthetized with 1% isoflurane and placed on a heating pad in the supine position to maintain a body temperature of 37°C to minimize the confounding effects of fluctuating body temperatures. Hair was removed using depilatory cream applied to the neck and stomach. The abdominal aorta was first visualized in brightness (B)-mode on the transverse plane. Aortic wall motion was then recorded in perpendicular orientation using M mode images captured at specific locations along the infrarenal aorta. Similar to the abdominal aorta, the carotid artery was first visualized on the transverse plane in B mode, and then the transducer was switched to obtain images on the longitudinal plane. Anterior and posterior aortic wall motion was assessed using images captured in M mode. Images were analyzed using the Vevo WorkStation. Systolic diameter (Ds) and diastolic diameter (Dd) were quantified from M mode images, and then circumferential cyclic strain was calculated as (Ds-Dd)/Dd.[27, 28] The aortic PWV was calculated as the distance between two measurement points divided by the time shift of the waveforms at the two points.[29] For the abdominal aorta, the blood flow and physiological signals were recorded along the abdominal aorta, focusing on two points, at the suprarenal branch and approximately 1 mm before the left renal artery branch. The time lag in blood flow at these two sites was measured between the R Wave in electrocardiography (ECG). Peak blood flow ($\Delta t1$, $\Delta t2$) time was recorded. $\Delta t1$ was the time lag in the low site (suprarenal) and $\Delta t2$ the time lag in the upper site (approximately 1 mm before the renal artery). The time required for the wave to go from the upper site to the low point provided the pulse transit time (PPT), calculated as follows: $PPT = \Delta T = \Delta t1 - \Delta t2$. The distance(S) travelled between these two sites was measured using color Doppler images. PWV was calculated as follows: $PWV=S/PPT= S/\Delta T = S/(\Delta t1 - \Delta t2)$. For the carotid artery, the blood flow was measured at two sites along left common carotid artery. One is at the common carotid, another is at the junction of the internal carotid artery derivatives and the external carotid artery derivatives. All echocardiography procedures, including data acquisition and analysis, were performed by a researcher blinded to the identity of the samples. Doppler spectrograms of aortic flow at the carotid artery and abdominal aortic site were acquired with a 20-MHz pulsed Doppler probe using the Vevo 3100 Imaging System.

SIRT1 activity analysis

To assess SIRT1 activity, a two-step enzymatic assay was utilized. First, assay procedure is based on a two-step enzymatic reaction. The first step is deacetylation by SIRT1 of a substrate that contains an acetylated lysine side chain. The second step is the cleavage of the deacetylated substrate by the Developing Solution and the release of a highly fluorescent group. The measured fluorescence is directly proportional to the deacetylation activity of the enzyme in the sample. A detailed description of the method is provided in the manufacturer’s instructions (Catalog # CS1040, Sigma-Aldrich, St. Louis, Missouri).

Site-directed mutagenesis of full-length *Sirt1* constructs

The full-length human *Sirt1* cDNA (clone 51746, Addgene, Cambridge, Massachusetts)[30] was sub-cloned into the pET-28a (+) vector using the restriction enzymes BamHI and SalI and *Sirt1*-specific oligonucleotide primers (forward, including BamHI restriction site: 5′-TATTAGGATCCATGGCGGACGAGGCG-3′; reverse, including SalI restriction site: 5′-GCGCGTCGACCTATGATTTGTTTGATGG −3′) and High-Fidelity DNA Polymerase (Invitrogen, Carlsbad, California). The authenticity of the inserts was confirmed by DNA sequencing at the Oklahoma Medical Research Facility DNA Sequencing Core facility using Applied Biosystems Big-Dye version 3.1 chemistry on an Applied Biosystems model 3730 automated capillary DNA Sequencer

Two *Sirt1* substitution mutations (C395S and C398S) were generated using the QuikChange II site-directed mutagenesis kit (Catalog # 200524, Agilent Technologies, Santa Clara, California) per manufacturer's instructions. The primers used to generate the mutants are as follows: Y280F forward primer: 5'-TCAAGGGATGGTATTTTTGCTCGCCTTGCTGTA-3', Y280F reverse primer: 5'-TACAGCAAGGCGAGCAAAAATACCATCCCTTGA-3'; C395S forward primer: 5'-CAGGTAGTTCCTCGATCTCCTAGGTGCCCAGCT-3', C395S reverse primer: 5'-AGCTGGGCACCTAGGAGATCGAGGAACTACCTG-3'; C398S forward primer: 5'-CCTCGATGTCCTAGGTCCCCAGCTGATGAACCG-3', C398S reverse primer: 5'-CGGTTCATCAGCTGGGGACCTAGGACATCGAGG-3'.

Mutations were verified by DNA sequencing at the Oklahoma Medical Research Facility DNA Sequencing Core facility as described above. Recombinant SIRT1 and SIRT1 mutant proteins were expressed in *E. coli* and purified using an affinity chromatography matrix Nickel-nitrilotriacetic acid (Ni-NTA) column under native condition.

Western blot analysis

Cell lysates were subjected to Western blot analysis to determine protein content. Whole aortas were collected, and after removal of the adventitia and endothelium, the liquid fraction of aortic wall homogenates was used for Western blot analysis. Protein content was measured using the Pierce™ BCA Protein Assay Kit (Thermo Fisher Scientific, Waltham, Massachusetts, USA). A total of 30 μg protein was loaded onto an SDS-PAGE gel and then transferred to a membrane. The membrane was incubated with primary antibody, followed by a horseradish peroxidase–conjugated secondary antibody.[26] Protein bands were visualized by enhanced chemiluminescence (ECL, Pierce Chemical Co.).

Quantification of *Sirt1* mRNA

Total RNA was extracted from hASMCs using the RNeasy Mini Kit (Qiagen, Hilden, Germany). Total RNA was extracted from murine aortas using the REzol C & T reagent from Protech Technology Enterprise CO., Ltd. (Taipei, Taiwan). Complementary DNA (cDNA) was transcribed using specific antisense primers with the ThermoScript™ RT-PCR System by Invitrogen (Carlsbad, California) per manufacturer's instructions, and mRNA concentration was determined using a SYBR green-based real-time quantitative RT-PCR assay (Applied Biosystems, Foster City, California). Primers used for RT-PCR are as

follows: Mouse *Sirt1* forward primer: 5'- GCTGACGACTTCGACGACG-3', Mouse *Sirt1* reverse primer: 5'-TCGGTCAACAGGAGGTTGTCT-3'. Human *Sirt1* forward primer: 5'-TAGCCTTGTCAGATAAGGAAGGA-3', Human *Sirt1* reverse primer: 5'-ACAGCTTCACAGTCAACTTTGT-3'. 18S rRNA forward primer: 5'-GTAACCCGTTGAACCCCATT-3', 18S rRNA reverse primer: 5'-CCATCCAATCGGTAGTAGCG-3'.

Detection of zinc release from SIRT1

Zinc (Zn^{2+}) release from purified recombinant human SIRT1 (Catalog # S8446, Sigma-Aldrich, St. Louis, Missouri) was measured via the PAR assay as described by Zou *et al.*[31] All assay buffers were pretreated with Chelex 100 (5 g/100 mL) to remove background Zn^{2+}. Then 100 μmol/L PAR was added to 1 mL of Chelex 100-pretreated Tris-HCl buffer (1 mol/L, pH 7.4) in a rapidly stirred cuvette at 25°C. The formation of the PAR2-Zn^{2+} complex was monitored by measuring absorbency at 500 nm with BioMate 3 Spectrophotometer from Thermo Scientific until no further increase was seen. At the end of the assay, 1 mmol/L nitrilotriacetic acid, which selectively chelates Zn^{2+}, was added to remove Zn^{2+} from the PAR2-Zn^{2+} complex. The resultant decrease in absorbance at 500 nm was used to quantify the total amount of Zn^{2+} released. The total Zn^{2+} content of untreated SIRT1 was quantified by determining maximal Zn^{2+} release by diluting SIRT1 proteins in 200 μL guanidine HCl (7 mol/L) pretreated with Chelex 100 and incubated for 30 minutes.

Statistical analyses

Results for PWV and strain are expressed as the mean ± SEM. All the other quantitative results are expressed as the mean ± SD. Normal distribution was confirmed via a Kolmogorov-Smirnov test and construction of Q-Q plots. Student's *t*-test and two-way ANOVA with Bonferroni correction were used to determine significant differences between two groups and between multiple groups, respectively. The *P*-value cutoff was 0.05.

Results

Nicotine induces arterial stiffness and ECM remodeling in mice

To assess the effect of nicotine on arterial stiffness, we infused eight-week-old wild-type (WT) mice with nicotine or vehicle (saline) via osmotic pump for four weeks while monitoring the motion (M)-mode of artery (Fig. 1A and B), circumferential cyclic strain, and PWV of the carotid artery via ultrasound. As shown in Fig. 1C and D, upper panel, nicotine significantly ($P<0.05$) decreased the circumferential cyclic strain in the carotid artery of male and female mice. Additionally, nicotine treatment was associated with significantly higher carotid artery PWV (Fig. 1C and D, bottom panel). These results together indicate that nicotine induces arterial stiffness in the carotid artery of both male and female mice.

To corroborate these observations, we next observed the morphology of the abdominal aorta (Fig. 1B). Similar to the carotid artery, nicotine treatment decreased abdominal aortic circumferential cyclic strain (Fig. 1C and D, upper panel) and increased PWV (Fig. 1C and D, bottom panel) in both male and female mice. The results indicate that there is no

significant difference of arterial stiffness between male and female mice with nicotine treatment. Then, we combined the data from male and female mice with all the following results. Interestingly, nicotine treatment also dramatically altered the extracellular matrix, leading to an accumulation of collagen (Fig. 1E), collagen I (Fig. 1F), and fibronectin (Fig. 1G), and enhanced elastin fragmentation (Fig. 1H).

Nicotine decreases SIRT1 protein levels and activity, but not mRNA levels, in both hASMCs and aortas

We next determined the effects of nicotine on the mRNA, protein levels and protein activity of SIRT1 in cultured human aortic smooth muscle cells (hASMCs) and in the aortas isolated from nicotine-infused mice. Nicotine treatment reduced the activity and protein levels of SIRT1 in both hASMCs (Fig. 2A and B) and isolated WT aortas (Fig. 2D and E) without affecting its mRNA levels (Fig. 2C and F), indicating that nicotine decreased SIRT1 stability.

Sirt1 overexpression attenuates nicotine-induced arterial stiffness

As shown in Fig. 3A and 3B, the protein expression levels and activity of SIRT1 in the aortas of $Sirt1^{Super}$ mice were three folds higher than those of WT mice. To further characterize the role of SIRT1 in nicotine-induced arterial stiffness, *Sirt1*-overexpressing ($Sirt1^{Super}$) mice, like WT mice, were infused with nicotine or vehicle. Nicotine reduced SIRT1 protein levels and activity in the aortas of $Sirt1^{Super}$ mice to the levels of SIRT1 in WT mice (Fig. 3A and 3B). We also measured M-mode and pulsed-wave (PW) mode, and then calculated circumferential cyclic strain and PWV of carotid arteries (Fig. 3C). Nicotine-induced decrease in circumferential cyclic strain in the carotid artery was significantly less in $Sirt1^{Super}$ mice than those in nicotine-treated WT mice (Fig. 3D). However, there was no significant difference in segmental PWV of the carotid artery between WT and $Sirt1^{Super}$ mice in the absence of nicotine treatment (Fig. 3E); Further, both M-mode and pulsed-wave (PW) mode were also used to calculate circumferential cyclic strain and PWV of abdominal aortas (Fig. 3F). As depicted in Fig. 3G, nicotine-induced reduction of the circumferential cyclic strain in the abdominal aorta were significantly less in $Sirt1^{Super}$ mice than their counterparts in nicotine-treated WT mice. The segmental PWV of the abdominal aorta between WT and $Sirt1^{Super}$ mice in the absence of nicotine treatment was also comparable (Fig. 3H); However, *Sirt1* overexpression attenuated the nicotine-induced increase in PWV in both the carotid arteries and abdominal aortas (Fig. 3E and H). Taken together, these results indicate that *Sirt1* overexpression attenuates nicotine-enhanced arterial stiffness in both the carotid artery and abdominal aorta.

Sirt1 overexpression alleviates nicotine-induced ECM remodeling

Because ECM remodeling contributes to arterial stiffness,[9, 32] we next determined whether *Sirt1* overexpression similarly blocks nicotine-induced ECM remodeling. In $Sirt1^{Super}$ mice, nicotine reduced SIRT1 protein levels to those in WT mice (Fig. 4A). Importantly, nicotine-induced increases in collagen I (Fig. 4B) and fibronectin (Fig. 4C) were significantly reduced in nicotine-treated $Sirt1^{Super}$ mice when compared to those in WT mice with nicotine treatment. Elastin breakage was also lower in nicotine-treated $Sirt1^{Super}$ mice than their counterparts in nicotine-treated WT mice (Fig. 4D). Finally, MMP2 expression was

dramatically decreased in aortas from nicotine-treated *Sirt1*^{Super} mice relative to that from nicotine-treated WT mice (Fig. 4E), indicating that *Sirt1* overexpression protects against nicotine-induced ECM remodeling, and further strengthening the protective role of *Sirt1* in nicotine-induced arterial stiffness.

Sirt1 overexpression mitigates nicotine-induced YAP activation

A key upstream effector of ECM remodeling is activation of the transcriptional co-activator Yes-associated protein (YAP)[33] via inhibition of phosphorylation of serine 127 (pYAP-S127);[34–36] therefore, we next determined whether nicotine treatment affects YAP activation. As shown in Fig. 5A, neither nicotine alone nor *Sirt1* overexpression alone altered total aortic YAP levels; however, nicotine markedly (P<0.01) decreased aortic pYAP-S127 levels, suggesting that nicotine induces YAP dephosphorylation and subsequent activation. Additionally, although *Sirt1* overexpression alone had no effect on YAP phosphorylation, *Sirt1* overexpression attenuated the nicotine-induced decrease in aortic pYAP-S127 (Fig. 5B), suggesting that SIRT1 inhibits nicotine-induced YAP activation.

Also, nicotine treatment decreased YAP phosphorylation in hASMCs in vitro (Fig. 5C and D) and increased YAP nuclear translocation (Online Fig. VI). Transfection of YAP siRNA in hASMCs dramatically decreased nicotine-enhanced collagen I protein levels when compared to those infected with control siRNA (Fig. 5C). Also, YAP siRNA markedly suppressed the nicotine-upregulated matrix metalloproteinases 2 (MMP2) contributing to elastin fragmentation,[37] compared to control siRNA (Fig. 5D). All these results suggest that YAP mediates the nicotine-induced extracellular matrix remodeling, including collagen accumulation and elastin breakage.

Nicotine increases reactive nitrogen species in murine aortas

Lastly we investigated the underlying mechanisms for SIRT1 inhibition by nicotine. Because elevated reactive oxygen species (ROS) are a hallmark of increased arterial stiffness and ECM remodeling,[21] we first validated that nicotine markedly enhanced the expression of inducible nitric oxide synthase (iNOS) in murine aortas (Fig. 6A). We then quantified $ONOO^-$, a potent oxidant generated from the reaction of superoxide anion ($O_2^{\cdot -}$) with nitric oxide (NO),[38] in murine aortas by measuring the biomarker 3-nitrotyrosine (3-NT).[39] Nicotine treatment significantly increased 3-NT levels in murine aortas (Fig. 6B), suggesting that nicotine indeed promotes the formation of $ONOO^-$. Importantly, strong co-staining of antibody against 3-NT and the antibody against SIRT1 in nicotine-treated murine aortas (Fig. 6C) further confirmed that SIRT1 is oxidized by nicotine-induced $ONOO^-$.

Tempol can effectively suppress $ONOO^-$ by scavenging superoxide anions.[40] Next, we tested if $ONOO^-$ was required for nicotine-induced SIRT1 inhibition and ECM remodeling. As expected, Tempol treatment repressed nicotine-enhanced 3-NT formation in the aorta (Fig. 6D). As depicted in Fig. 6E and 6F, co-administration of Tempol with nicotine prevented nicotine-induced reduction of SIRT1 protein and its activity, as well as pYAP in mouse aorta. Also, Tempol ablated nicotine-induced collagen induction (visualized by Masson trichrome staining in Fig. 6G and quantified by aorta hydroxyproline assay[41] in

Online Fig. VII). Taken together, these data imply that scavenging $ONOO^-$ prevents SIRT1 inhibition with consequent collagen upregulation in nicotine-infused mice.

$ONOO^-$-mediated SIRT1 inhibition

Finally, we sought to determine whether the mechanism behind nicotine-induced SIRT1 inhibition was dependent on nicotine-induced ROS. Because zinc binding is critical for the catalytic activity of SIRT1,[42] we determined whether $ONOO^-$ inhibits SIRT1 by causing zinc release and thereby inactivating the protein. As shown in Fig. 7A, $ONOO^-$ inhibited the activity of human recombinant SIRT1 in a dose-dependent manner, and indeed, depleted SIRT1-bound zinc up to 62% ± 8% of maximal release. In contract, decomposed $ONOO^-$ ($dONOO^-$) depleted SIRT1-bound zinc up to only 5%, strongly suggesting that $ONOO^-$-induced SIRT1 inhibition is a direct result of zinc release. Then, we want to know whether supplement of exogenous zinc recovers SIRT1 activity inhibited by $ONOO^-$. As expected, exogenous zinc did not block $ONOO^-$-mediated inhibition of SIRT1 activity, while zinc chloride ($ZnCl_2$) enhanced the $ONOO^-$-mediated SIRT1 inhibition (Fig. 7C). These data together strongly suggest that zinc release is irreversible and exogenous zinc directly inhibits SIRT1 catalytic activity independently of the zinc-thiolate complex, corroborating the results reported by Chen *et al.*[43]

As zinc and four cysteine residues in SIRT1 form zinc-tetrathiolate center (C371LIC374-$(X)_{20}$-C395PRC398), which is required for the structure integrity and bioactivity of SIRT1,[42] we further mutated single cysteine residue in zinc-tetrathiolate center of SIRT1. As shown in Fig. 7D, either cysteine 395 mutation to serine (C395S) or C398S mutation totally blocked SIRT1 activity under basal condition. Because tyrosine 280 side chain hydroxyl of SIRT1 is crucial for its substrate NAD^+ binding,[44] we then mutated tyrosine 280 to phenylalanine (Y280F) in SIRT1 and found Y280F mutation significantly impaired SIRT1 activity under basal condition (Fig. 7D).

Discussion

In this study, we have described a novel mechanism, i.e., nicotine via $ONOO^-$ -induced SIRT1 inhibition instigates arterial stiffness *in vivo*. Specifically, we found that nicotine increases the formation of $ONOO^-$, which attacks the zinc-tetrathiolate center of SIRT1, resulting in zinc release and the enzymatic inhibition of SIRT1 deacetylase activity. As a result, YAP is activated, inducing collagen and fibronectin formation, as well as elastin fragmentation mediated by MMP2 upregulation, ultimately leading to ECM remodeling (Fig. 7E). Altogether, we demonstrate that nicotine potentiates arterial stiffness through ECM remodeling. Notably, collagen levels significantly increased in murine aortas upon nicotine treatment, a significant observation given that elevated collagen directly contributes to the increased arterial stiffness. This corroborates prior work demonstrating that ECM disorganization results in increased abdominal aortic stiffness in aged monkeys.[6]

Deregulated SIRT1 is widely reported to be involved in vascular remodeling and arterial stiffness although a causative role remains to be established. For example, aortas from angiotensin II–treated VSMC-specific *Sirt1* knockout mice have severely disarrayed elastic lamellae with more elastin fragments and increased aortic stiffness.[45] Furthermore,

resveratrol, a strong SIRT1 activator, prevents high fat/sucrose diet-induced central arterial wall remodeling and stiffening in mice and in rhesus monkeys.[46] Here, we demonstrate a direct connection between SIRT1 and nicotine-induced arterial stiffness. Nicotine not only enhanced arterial stiffness in mice, but also decreased SIRT1 protein levels and activity both in murine aortas and in hASMCs, while *Sirt1* overexpression fully attenuated nicotine-induced arterial stiffness. Nicotine exposure instigates arterial stiffness and the chronical arterial stiffness is reported to cause hypertension.[2, 47] However, Fry JL et al showed that smooth muscle SIRT1 regulates ECM remodeling and protects against angiotensin II-induced aneurysm formation, which is independent of hypertension.[45] In the present study, nicotine treatment for 4 weeks increased arterial stiffness, but had no effect on blood pressure (data not shown). The results suggest that short-term arterial stiffness alone is not enough to induce high blood pressure, which is consistent with the report that arterial stiffening (develops within 1 month of the initiation of diet) precedes systolic hypertension (develops by 6 months) in high-fat/high-sucrose diet-induced obesity.[47] These results highlight SIRT1 as a promising target for the development of new treatments for arterial stiffness. Indeed, numerous studies indicate that *Sirt1* activation represents an attractive therapeutic approach against arterial stiffness and subsequent adverse cardiovascular events.[48, 49]

There are several mechanisms by which SIRT1 could be manipulated. Protein levels are regulated by several transcriptions factors and can also be modified through microRNA. Additionally, the protein can be cleaved by cathepsin[50] or caspase 1,[51] and is affected by several post-translational modifications, including phosphorylation, methylation, SUMOylation, and nitrosylation.[52, 53] Here, we focus on the redox post-translational modification of SIRT1, which is only recently gaining recognition.[53, 54] The zinc-tetrathiolate center of SIRT1 is critical for the structural integrity and deacetylase activity of the protein.[43] We found that exogenous $ONOO^-$ inhibited the activity of human recombinant SIRT1 in a dose-dependent manner. Simultaneously, $ONOO^-$ promoted zinc release from the recombinant SIRT1. Most importantly, site-directed mutagenesis of the zinc-binding cysteine residues of zinc-tetrathiolate center in SIRT1 abolished its activity. Finally, inhibition of $ONOO^-$ with Tempol markedly protected the nicotine-induced SIRT1 inhibition and aortic ECM remodeling. Altogether, our results support the notion that $ONOO^-$ directly attacks the thiolate group of cysteines within zinc-tetrathiolate center. However, it is inapplicable to detect zinc release from SIRT1 in vivo or in VSMC in vitro, because there are numerous enzymes or protein including inducible nitric-oxide synthases (NOS)[55] and MMPs[56] beside SIRT1 contain oxidants-sensitive zinc.

$ONOO^-$ is a potent oxidant which is able to cause multiple forms of protein posttranslational modifications including tyrosine nitration,[57] S-nitrosylation,[58] S-glutathiolation,[59] etc. Interestingly, nicotine exposure increased SIRT1 tyrosine nitration (SIRT1 and 3-NT co-staining in aorta), suggesting nicotine may increase SIRT1 tyrosine nitration. SIRT1 substrate NAD^+ terminal amide hydrogen bonds to the Y280 side chain hydroxyl of SIRT1.[44] SIRT1 Y280F mutation remarkably inhibited SIRT1 activity (Fig. 7D). All these data suggest that Y280 of SIRT1 may be the key tyrosine-nitrated site and required for SIRT1 activity. Further study is warranted. Although we found high concentrations (μM) of

$ONOO^-$ releases zinc from SIRT1, it remains possible that $ONOO^-$ suppress SIRT1 activity by various mechanisms, depending upon the concentrations and exposure time of $ONOO^-$.

Our results suggest that SIRT1 ablates arterial stiffness via inhibition of YAP-mediated ECM remodeling. Protein deacetylase SIRT1 has been reported to be responsible for YAP deacetylation,[34, 60] which increases YAP phosphorylation, blocks the nuclear translocation of YAP, and subsequently inactivates YAP in HeLa cancer cells[34] and esophageal squamous cancer cell.[61] Consistent with these observations, we found that nicotine decreased SIRT1 protein levels and resultant YAP dephosphorylation, while SIRT1 overexpression abolished nicotine-suppressed YAP phosphorylation as well as YAP inactivation-instigated effects in VSMC. Further, YAP knockdown by specific siRNA blocked the collagen I and MMP2 upregulation by nicotine. All these results suggest that SIRT1 inhibits YAP via induction of YAP phosphorylation and negatively regulates extracellular matrix remodeling by YAP-mediated collagen I and MMP2 upregulation. However, YAP deacetylation and its function regulated by SIRT1 in VSMC warrant further investigation. As YAP function is required for the elevated matrix stiffening[33] and stiff matrices will further activate YAP signaling,[33, 62, 63] YAP inhibition might be a valid therapeutic target for treating arterial stiffness and arteriosclerosis.

In summary, our study has demonstrated that nicotine exposure triggers arterial stiffness via SIRT1 inhibition-mediated YAP activation. As the nicotine administration is widely used in smoking cessation, nicotine replacement therapy should be cautiously used in smokers with established cardiovascular diseases such as hypertension, heart failure, etc.

Supplementary Material

Refer to Web version on PubMed Central for supplementary material.

Acknowledgements

Sources of Funding

This study was supported in part by the following grants: NHLBI (HL079584, HL080499, HL089920, HL110488, HL128014, HL132500, HL137371, and HL140954), NCI (CA213022), NIA (AG047776). Dr. M.H. Zou is an eminent scholar of the Georgia Research Alliance. Dr. Y. Ding was supported by postdoctoral fellowship award (16POST31160009) from American Heart Association.

Nonstandard Abbreviations and Acronyms

3-NT	3-nitrotyrosine
ECM	extracellular matrix
$ONOO^-$	peroxynitrite
PWV	pulse-wave velocity
SIRT1	Sirtuin-1
$Sirt1^{Super}$	*Sirt1*-overexpressing

YAP	Yes-associated protein

References

1. Huveneers S, Daemen MJ, Hordijk PL. Between rho(k) and a hard place: The relation between vessel wall stiffness, endothelial contractility, and cardiovascular disease. Circ Res. 2015;116:895–908. [PubMed: 25722443]
2. Kaess BM, Rong J, Larson MG, Hamburg NM, Vita JA, Levy D, Benjamin EJ, Vasan RS, Mitchell GF. Aortic stiffness, blood pressure progression, and incident hypertension. JAMA. 2012;308:875–881. [PubMed: 22948697]
3. Pandey A, Khan H, Newman AB, Lakatta EG, Forman DE, Butler J, Berry JD. Arterial stiffness and risk of overall heart failure, heart failure with preserved ejection fraction, and heart failure with reduced ejection fraction: The health abc study (health, aging, and body composition). Hypertension. 2017;69:267–274. [PubMed: 27993954]
4. Pase MP, Beiser A, Himali JJ, Tsao C, Satizabal CL, Vasan RS, Seshadri S, Mitchell GF. Aortic stiffness and the risk of incident mild cognitive impairment and dementia. Stroke. 2016;47:2256–2261. [PubMed: 27491735]
5. Safar ME, London GM, Plante GE. Arterial stiffness, kidney function. Hypertension. 2004;43:163–168. [PubMed: 14732732]
6. Zhang J, Zhao X, Vatner DE, McNulty T, Bishop S, Sun Z, Shen YT, Chen L, Meininger GA, Vatner SF. Extracellular matrix disarray as a mechanism for greater abdominal versus thoracic aortic stiffness with aging in primates. Arterioscler Thromb Vasc Biol. 2016;36:700–706. [PubMed: 26891739]
7. Venkatasubramanian S, Noh RM, Daga S, Langrish JP, Mills NL, Waterhouse BR, Hoffmann E, Jacobson EW, Lang NN, Frier BM, Newby DE. Effects of the small molecule sirt1 activator, srt2104 on arterial stiffness in otherwise healthy cigarette smokers and subjects with type 2 diabetes mellitus. Open Heart. 2016;3:e000402. [PubMed: 27239324]
8. Xu M, Huang Y, Xie L, Peng K, Ding L, Lin L, Wang P, Hao M, Chen Y, Sun Y, Qi L, Wang W, Ning G, Bi Y. Diabetes and risk of arterial stiffness: A mendelian randomization analysis. Diabetes. 2016;65:1731–1740. [PubMed: 26953161]
9. Chen JY, Tsai PJ, Tai HC, et al. Increased aortic stiffness and attenuated lysyl oxidase activity in obesity. Arterioscler Thromb Vasc Biol. 2013;33:839–846. [PubMed: 23413430]
10. Canepa M, Viazzi F, Strait JB, Ameri P, Pontremoli R, Brunelli C, Studenski S, Ferrucci L, Lakatta EG, AlGhatrif M. Longitudinal association between serum uric acid and arterial stiffness: Results from the baltimore longitudinal study of aging. Hypertension. 2017;69:228–235. [PubMed: 27956574]
11. Mahmud A, Feely J. Effect of smoking on arterial stiffness and pulse pressure amplification. Hypertension. 2003;41:183–187. [PubMed: 12511550]
12. Rhee MY, Na SH, Kim YK, Lee MM, Kim HY. Acute effects of cigarette smoking on arterial stiffness and blood pressure in male smokers with hypertension. Am J Hypertens. 2007;20:637–641. [PubMed: 17531920]
13. Jatoi NA, Jerrard-Dunne P, Feely J, Mahmud A. Impact of smoking and smoking cessation on arterial stiffness and aortic wave reflection in hypertension. Hypertension. 2007;49:981–985. [PubMed: 17372029]
14. Benowitz NL. Cigarette smoking and cardiovascular disease: Pathophysiology and implications for treatment. Progress in cardiovascular diseases. 2003;46:91–111. [PubMed: 12920702]
15. Adamopoulos D, Argacha JF, Gujic M, Preumont N, Degaute JP, van de Borne P. Acute effects of nicotine on arterial stiffness and wave reflection in healthy young non-smokers. Clin Exp Pharmacol Physiol. 2009;36:784–789. [PubMed: 19207722]
16. Vlachopoulos C, Ioakeimidis N, Abdelrasoul M, Terentes-Printzios D, Georgakopoulos C, Pietri P, Stefanadis C, Tousoulis D. Electronic cigarette smoking increases aortic stiffness and blood pressure in young smokers. J Am Coll Cardiol. 2016;67:2802–2803. [PubMed: 27282901]

17. Sehgel NL, Zhu Y, Sun Z, Trzeciakowski JP, Hong Z, Hunter WC, Vatner DE, Meininger GA, Vatner SF. Increased vascular smooth muscle cell stiffness: A novel mechanism for aortic stiffness in hypertension. Am J Physiol Heart Circ Physiol. 2013;305:H1281–1287. [PubMed: 23709594]
18. Lacolley P, Regnault V, Segers P, Laurent S. Vascular smooth muscle cells and arterial stiffening: Relevance in development, aging, and disease. Physiol Rev. 2017;97:1555–1617. [PubMed: 28954852]
19. Li L, Zhang HN, Chen HZ, et al. Sirt1 acts as a modulator of neointima formation following vascular injury in mice. Circ Res. 2011;108:1180–1189. [PubMed: 21474819]
20. Chen HZ, Wang F, Gao P, et al. Age-associated sirtuin 1 reduction in vascular smooth muscle links vascular senescence and inflammation to abdominal aortic aneurysm. Circ Res. 2016;119:1076–1088. [PubMed: 27650558]
21. Fry JL, Al Sayah L, Weisbrod RM, Van Roy I, Weng X, Cohen RA, Bachschmid MM, Seta F. Vascular smooth muscle sirtuin-1 protects against diet-induced aortic stiffness. Hypertension. 2016;68:775–784. [PubMed: 27432859]
22. Zieman SJ, Melenovsky V, Kass DA. Mechanisms, pathophysiology, and therapy of arterial stiffness. Arterioscler Thromb Vasc Biol. 2005;25:932–943. [PubMed: 15731494]
23. Pfluger PT, Herranz D, Velasco-Miguel S, Serrano M, Tschop MH. Sirt1 protects against high-fat diet-induced metabolic damage. Proc Natl Acad Sci U S A. 2008;105:9793–9798. [PubMed: 18599449]
24. Wang Q, Ding Y, Song P, Zhu H, Okon I, Ding YN, Chen HZ, Liu DP, Zou MH. Tryptophan-derived 3-hydroxyanthranilic acid contributes to angiotensin ii-induced abdominal aortic aneurysm formation in mice in vivo. Circulation. 2017;136:2271–2283. [PubMed: 28978552]
25. Yamato M, Kawano K, Yamanaka Y, Saiga M, Yamada K. Tempol increases nad(+) and improves redox imbalance in obese mice. Redox Biol. 2016;8:316–322. [PubMed: 26942863]
26. Ding Y, Zhang M, Zhang W, Lu Q, Cai Z, Song P, Okon IS, Xiao L, Zou MH. Amp-activated protein kinase alpha 2 deletion induces vsmc phenotypic switching and reduces features of atherosclerotic plaque stability. Circ Res. 2016;119:718–730. [PubMed: 27439892]
27. Prakash A, Adlakha H, Rabideau N, Hass CJ, Morris SA, Geva T, Gauvreau K, Singh MN, Lacro RV. Segmental aortic stiffness in children and young adults with connective tissue disorders: Relationships with age, aortic size, rate of dilation, and surgical root replacement. Circulation. 2015;132:595–602. [PubMed: 26115544]
28. Raaz U, Zollner AM, Schellinger IN, et al. Segmental aortic stiffening contributes to experimental abdominal aortic aneurysm development. Circulation. 2015;131:1783–1795. [PubMed: 25904646]
29. Williams R, Needles A, Cherin E, Zhou YQ, Henkelman RM, Adamson SL, Foster FS. Noninvasive ultrasonic measurement of regional and local pulse-wave velocity in mice. Ultrasound Med Biol. 2007;33:1368–1375. [PubMed: 17561330]
30. Ralser M, Zeidler U, Lehrach H. Interfering with glycolysis causes sir2-dependent hyper-recombination of saccharomyces cerevisiae plasmids. PLoS One. 2009;4:e5376. [PubMed: 19390637]
31. Zou MH, Shi C, Cohen RA. Oxidation of the zinc-thiolate complex and uncoupling of endothelial nitric oxide synthase by peroxynitrite. J Clin Invest. 2002;109:817–826. [PubMed: 11901190]
32. Lorentzen KA, Chai S, Chen H, Danielsen CC, Simonsen U, Wogensen L. Mechanisms involved in extracellular matrix remodeling and arterial stiffness induced by hyaluronan accumulation. Atherosclerosis. 2016;244:195–203. [PubMed: 26671518]
33. Calvo F, Ege N, Grande-Garcia A, Hooper S, Jenkins RP, Chaudhry SI, Harrington K, Williamson P, Moeendarbary E, Charras G, Sahai E. Mechanotransduction and yap-dependent matrix remodelling is required for the generation and maintenance of cancer-associated fibroblasts. Nat Cell Biol. 2013;15:637–646. [PubMed: 23708000]
34. Hata S, Hirayama J, Kajiho H, Nakagawa K, Hata Y, Katada T, Furutani-Seiki M, Nishina H. A novel acetylation cycle of transcription co-activator yes-associated protein that is downstream of hippo pathway is triggered in response to sn2 alkylating agents. J Biol Chem. 2012;287:22089–22098. [PubMed: 22544757]

35. Kimura TE, Duggirala A, Smith MC, White S, Sala-Newby GB, Newby AC, Bond M. The hippo pathway mediates inhibition of vascular smooth muscle cell proliferation by camp. J Mol Cell Cardiol. 2016;90:1–10. [PubMed: 26625714]
36. He C, Lv X, Huang C, Angeletti PC, Hua G, Dong J, Zhou J, Wang Z, Ma B, Chen X, Lambert PF, Rueda BR, Davis JS, Wang C. A human papillomavirus-independent cervical cancer animal model reveals unconventional mechanisms of cervical carcinogenesis. Cell reports. 2019;26:2636–2650 e5. [PubMed: 30840887]
37. Duca L, Blaise S, Romier B, Laffargue M, Gayral S, El Btaouri H, Kawecki C, Guillot A, Martiny L, Debelle L, Maurice P. Matrix ageing and vascular impacts: Focus on elastin fragmentation. Cardiovasc Res. 2016;110:298–308. [PubMed: 27009176]
38. Radi R Protein tyrosine nitration: Biochemical mechanisms and structural basis of functional effects. Acc Chem Res. 2013;46:550–559. [PubMed: 23157446]
39. Song P, Wu Y, Xu J, Xie Z, Dong Y, Zhang M, Zou MH. Reactive nitrogen species induced by hyperglycemia suppresses akt signaling and triggers apoptosis by upregulating phosphatase pten (phosphatase and tensin homologue deleted on chromosome 10) in an lkb1-dependent manner. Circulation. 2007;116:1585–1595. [PubMed: 17875968]
40. Carroll RT, Galatsis P, Borosky S, Kopec KK, Kumar V, Althaus JS, Hall ED. 4-hydroxy-2,2,6,6-tetramethylpiperidine-1-oxyl (tempol) inhibits peroxynitrite-mediated phenol nitration. Chem Res Toxicol. 2000;13:294–300. [PubMed: 10775330]
41. Wu J, Thabet SR, Kirabo A, Trott DW, Saleh MA, Xiao L, Madhur MS, Chen W, Harrison DG. Inflammation and mechanical stretch promote aortic stiffening in hypertension through activation of p38 mitogen-activated protein kinase. Circ Res. 2014;114:616–625. [PubMed: 24347665]
42. Min J, Landry J, Sternglanz R, Xu RM. Crystal structure of a sir2 homolog-nad complex. Cell. 2001;105:269–279. [PubMed: 11336676]
43. Chen L, Feng Y, Zhou Y, Zhu W, Shen X, Chen K, Jiang H, Liu D. Dual role of zn2+ in maintaining structural integrity and suppressing deacetylase activity of sirt1. Journal of inorganic biochemistry. 2010;104:180–185. [PubMed: 19923004]
44. Zhao X, Allison D, Condon B, Zhang F, Gheyi T, Zhang A, Ashok S, Russell M, Macewan I, Qian Y, Jamison JA, Luz JG. The 2.5 a crystal structure of the sirt1 catalytic domain bound to nicotinamide adenine dinucleotide (nad(+)) and an indole (ex527 analogue) reveals a novel mechanism of histone deacetylase inhibition. Journal of medicinal chemistry. 2013;56:963–969. [PubMed: 23311358]
45. Fry JL, Shiraishi Y, Turcotte R, Yu X, Gao YZ, Akiki R, Bachschmid M, Zhang Y, Morgan KG, Cohen RA, Seta F. Vascular smooth muscle sirtuin-1 protects against aortic dissection during angiotensin ii-induced hypertension. Journal of the American Heart Association. 2015;4:e002384. [PubMed: 26376991]
46. Mattison JA, Wang M, Bernier M, et al. Resveratrol prevents high fat/sucrose diet-induced central arterial wall inflammation and stiffening in nonhuman primates. Cell Metab. 2014;20:183–190. [PubMed: 24882067]
47. Weisbrod RM, Shiang T, Al Sayah L, Fry JL, Bajpai S, Reinhart-King CA, Lob HE, Santhanam L, Mitchell G, Cohen RA, Seta F. Arterial stiffening precedes systolic hypertension in diet-induced obesity. Hypertension. 2013;62:1105–1110. [PubMed: 24060894]
48. Bai B, Man AW, Yang K, Guo Y, Xu C, Tse HF, Han W, Bloksgaard M, De Mey JG, Vanhoutte PM, Xu A, Wang Y. Endothelial sirt1 prevents adverse arterial remodeling by facilitating herc2-mediated degradation of acetylated lkb1. Oncotarget. 2016;7:39065–39081. [PubMed: 27259994]
49. Gao D, Zuo Z, Tian J, Ali Q, Lin Y, Lei H, Sun Z. Activation of sirt1 attenuates klotho deficiency-induced arterial stiffness and hypertension by enhancing amp-activated protein kinase activity. Hypertension. 2016;68:1191–1199. [PubMed: 27620389]
50. Chen J, Xavier S, Moskowitz-Kassai E, Chen R, Lu CY, Sanduski K, Spes A, Turk B, Goligorsky MS. Cathepsin cleavage of sirtuin 1 in endothelial progenitor cells mediates stress-induced premature senescence. Am J Pathol. 2012;180:973–983. [PubMed: 22234173]
51. Chalkiadaki A, Guarente L. High-fat diet triggers inflammation-induced cleavage of sirt1 in adipose tissue to promote metabolic dysfunction. Cell Metab. 2012;16:180–188. [PubMed: 22883230]

52. Revollo JR, Li X. The ways and means that fine tune sirt1 activity. Trends in biochemical sciences. 2013;38:160–167. [PubMed: 23394938]

53. Kalous KS, Wynia-Smith SL, Olp MD, Smith BC. Mechanism of sirt1 nad+-dependent protein deacetylase inhibition by cysteine s-nitrosation. J Biol Chem. 2016;291:25398–25410. [PubMed: 27756843]

54. Caito S, Rajendrasozhan S, Cook S, Chung S, Yao H, Friedman AE, Brookes PS, Rahman I. Sirt1 is a redox-sensitive deacetylase that is post-translationally modified by oxidants and carbonyl stress. FASEB J. 2010;24:3145–3159. [PubMed: 20385619]

55. Li H, Raman CS, Glaser CB, Blasko E, Young TA, Parkinson JF, Whitlow M, Poulos TL. Crystal structures of zinc-free and -bound heme domain of human inducible nitric-oxide synthase. Implications for dimer stability and comparison with endothelial nitric-oxide synthase. J Biol Chem. 1999;274:21276–21284. [PubMed: 10409685]

56. Klein T, Bischoff R. Physiology and pathophysiology of matrix metalloproteases. Amino Acids. 2011;41:271–290. [PubMed: 20640864]

57. Zou MH, Shi C, Cohen RA. High glucose via peroxynitrite causes tyrosine nitration and inactivation of prostacyclin synthase that is associated with thromboxane/prostaglandin h(2) receptor-mediated apoptosis and adhesion molecule expression in cultured human aortic endothelial cells. Diabetes. 2002;51:198–203. [PubMed: 11756341]

58. Viner RI, Williams TD, Schoneich C. Peroxynitrite modification of protein thiols: Oxidation, nitrosylation, and s-glutathiolation of functionally important cysteine residue(s) in the sarcoplasmic reticulum ca-atpase. Biochemistry. 1999;38:12408–12415. [PubMed: 10493809]

59. Adachi T, Weisbrod RM, Pimentel DR, Ying J, Sharov VS, Schoneich C, Cohen RA. S-glutathiolation by peroxynitrite activates serca during arterial relaxation by nitric oxide. Nat Med. 2004;10:1200–1207. [PubMed: 15489859]

60. Mao B, Hu F, Cheng J, Wang P, Xu M, Yuan F, Meng S, Wang Y, Yuan Z, Bi W. Sirt1 regulates yap2-mediated cell proliferation and chemoresistance in hepatocellular carcinoma. Oncogene. 2014;33:1468–1474. [PubMed: 23542177]

61. Zhao Y, Zhou W, Xue L, Zhang W, Zhan Q. Nicotine activates yap1 through nachrs mediated signaling in esophageal squamous cell cancer (escc). PLoS One. 2014;9:e90836. [PubMed: 24621512]

62. Price AJ, Huang EY, Sebastiano V, Dunn AR. A semi-interpenetrating network of polyacrylamide and recombinant basement membrane allows pluripotent cell culture in a soft, ligand-rich microenvironment. Biomaterials. 2017;121:179–192. [PubMed: 28088685]

63. Nukuda A, Sasaki C, Ishihara S, Mizutani T, Nakamura K, Ayabe T, Kawabata K, Haga H. Stiff substrates increase yap-signaling-mediated matrix metalloproteinase-7 expression. Oncogenesis. 2015;4:e165. [PubMed: 26344692]

Highlights

- *Sirt1* overexpression ameliorates nicotine-induced arterial stiffness.
- Nicotine inhibits SIRT1 activity in mouse aorta and human aortic smooth muscle cells.
- Nicotine enhances extracellular matrix remodeling via SIRT1 inhibition-mediated activation of Yes-associated protein.
- Peroxynitrite-mediated zinc release contributes to SIRT1 inhibition by nicotine.

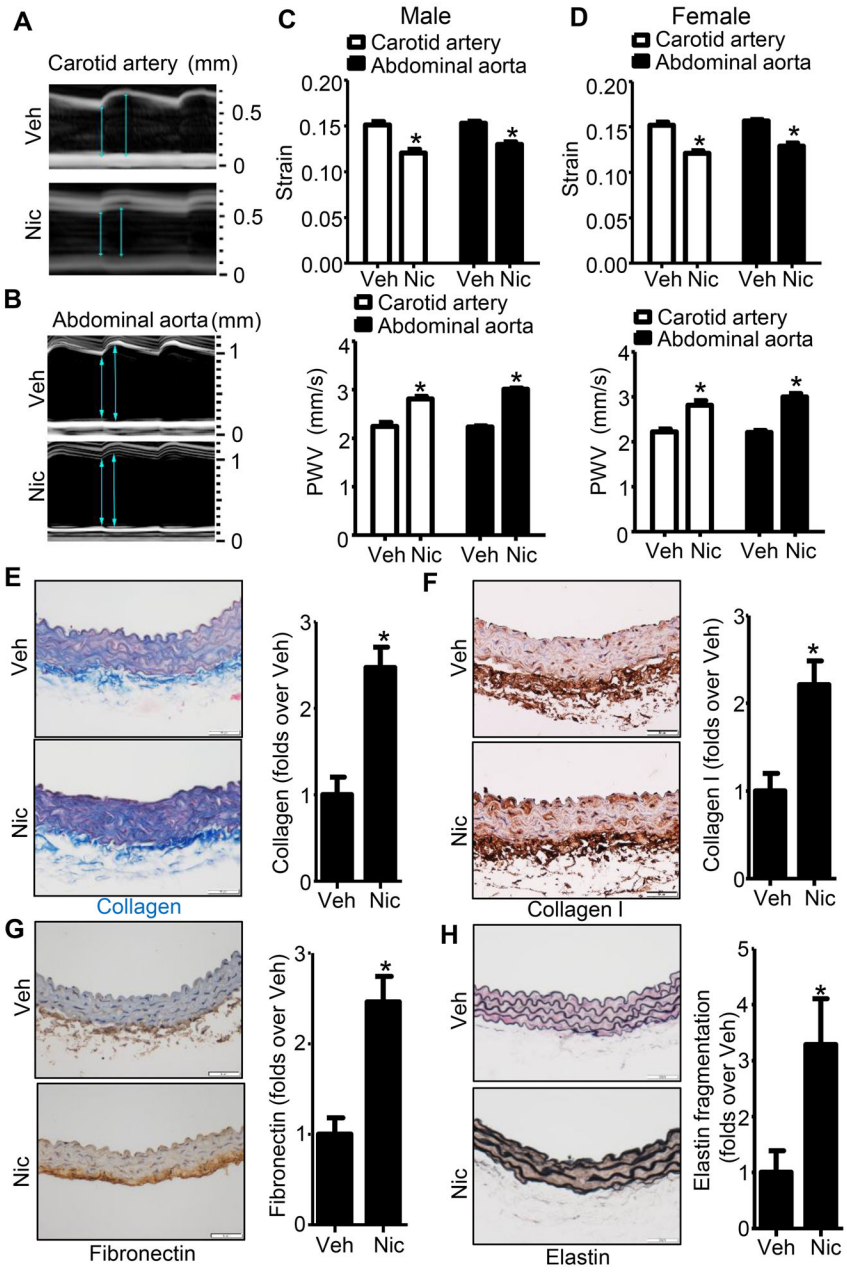

Figure 1. Nicotine induces arterial stiffness and remodeling of extracellular matrix in mice.

A. Representative images of motion (M)-mode for carotid artery monitored by ultrasound from vehicle- or nicotine-treated mice. **B**. Representative images of M-mode for abdominal aorta monitored by ultrasound from vehicle- or nicotine-treated mice. **C**. Circumferential cyclic strain (upper panel) and analysis of segmental stiffness (lower panel) of carotid artery and abdominal aorta in vehicle- or nicotine-treated male mice (n=5; * $P < 0.05$ *vs.* Veh). **D**. Circumferential cyclic strain (upper panel) and analysis of segmental stiffness (lower panel) of carotid artery and abdominal aorta in vehicle- or nicotine-treated female mice (n=5; * $P <$ 0.05 *vs.* Veh). **E**. Representative images and quantification of collagen content in aorta based on Masson trichrome staining (Blue color) of vehicle- or nicotine-treated mice (n=5; * $P <$

0.05 *vs.* Veh). **F**. Representative images and quantification of collagen I in aorta based on IHC staining of vehicle- or nicotine-treated mice (n=5; * $P < 0.05$ *vs.* Veh). **G**. Representative images and quantification of fibronectin in aorta based on IHC staining of vehicle- or nicotine-treated mice (n=5; * $P < 0.05$ *vs.* Veh). **H**. Representative images and quantification of elastin fragmentation in aorta based on Van Gieson's staining of vehicle- or nicotine-treated mice (n=5; * $P < 0.05$ *vs.* Veh). Veh, vehicle; Nic, nicotine. Negative controls for anti-Collagen I staining and anti-Fibronectin staining were presented in Online Figure I.

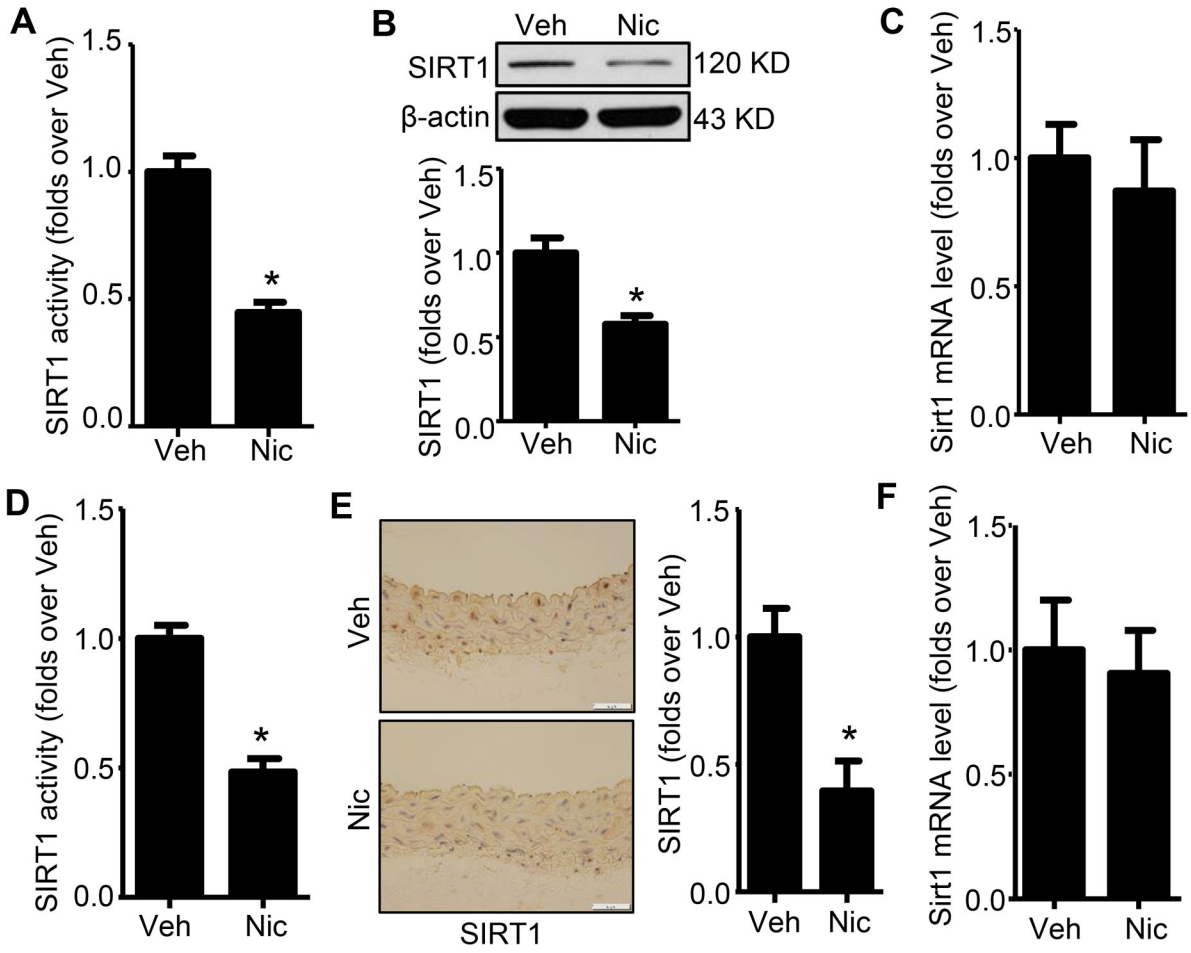

Figure 2. Nicotine reduces SIRT1 activity and protein expression in both cultured hASMCs and aorta.

A. SIRT1 activity was measured from hASMCs nuclear extracts. Data was normalized to the activity measured in vehicle-treated hASMCs (n=5; * $P < 0.05$ *vs.* Veh). **B**. Western blot analysis of SIRT1 protein expression in hASMCs treated with vehicle or nicotine for 24h (n=5; * $P < 0.05$ *vs.* Veh). **C**. Quantitative real-time PCR of *Sirt1* in hASMCs treated with vehicle or nicotine for 24h (n=3). **D**. SIRT1 activity was measured from aorta nuclear extracts. Data were normalized to the activity measured in vehicle-treated mice (n=5; * $P < 0.05$ *vs.* Veh). **E**. Representative images of IHC staining and quantification of SIRT1 in the aorta from vehicle- and nicotine-treated mice (n=5; * $P < 0.05$ *vs.* Veh). **F**. Quantitative real-time PCR of *Sirt1* in aorta from vehicle- and nicotine-treated mice (n=3). Veh, vehicle; Nic, nicotine. Negative control for anti-SIRT1 staining was presented in Online Figure II.

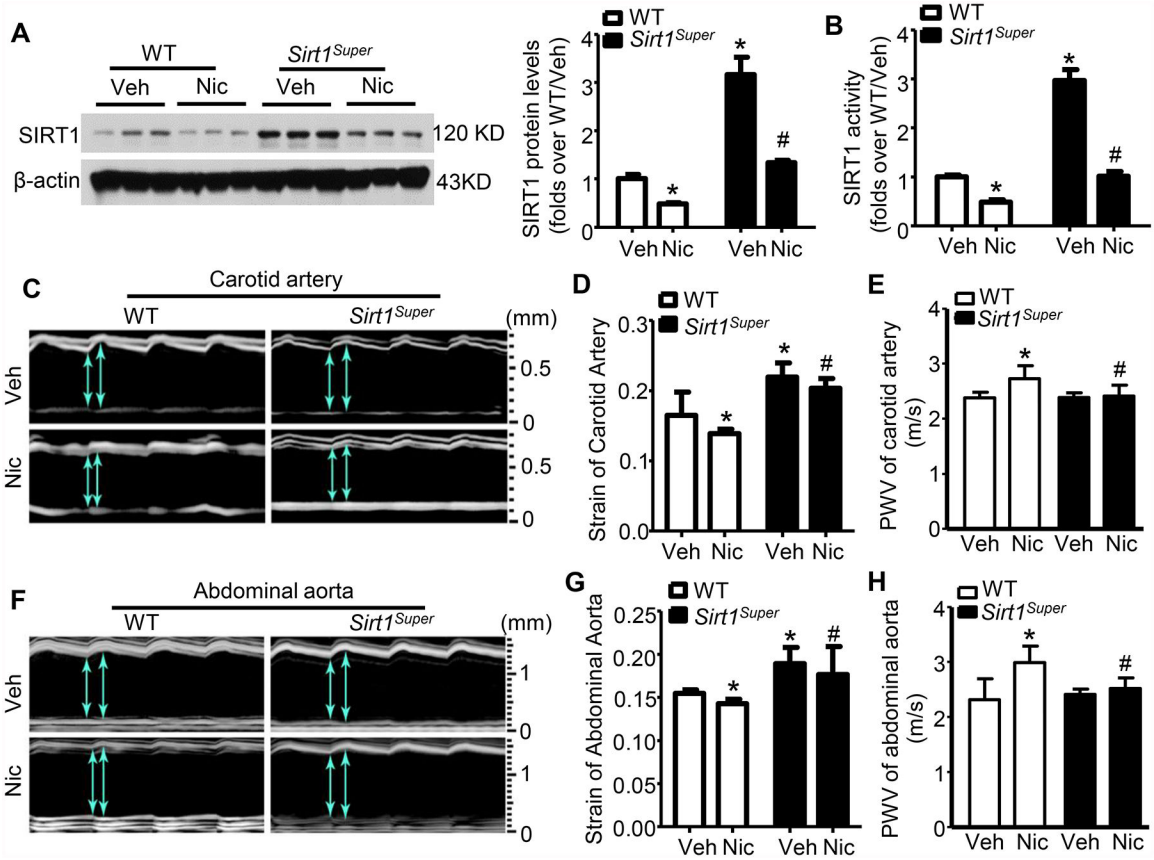

Figure 3. *Sirt1* overexpression eliminates nicotine-induced arterial stiffness.

A. Western blot analysis of SIRT1 protein expression in aortas from WT and *Sirt1*-overexpressing (*Sirt1*^{Super}) mice treated with vehicle or nicotine for 4 weeks (n=5; * $P <$ 0.05 *vs.* WT/Veh; $^{\#}$ $P < 0.05$ *vs.* WT/Nic). **B**. SIRT1 activity was measured from aorta nuclear extracts. Data were normalized to the activity measured in vehicle-treated WT mice (n=5; * $P < 0.05$ *vs.* WT/Veh; $^{\#}$ $P < 0.05$ *vs.* WT/Nic). **C**. Representative images of motion (M)-mode for carotid artery monitored by ultrasound from WT and *Sirt1*^{Super} mice treated with/without nicotine. **D**. Circumferential cyclic strain of carotid artery in WT and *Sirt1*^{Super} mice with/without nicotine treatment (n=10; * $P < 0.05$ *vs.* WT/Veh; # $P < 0.05$ *vs.* WT/Nic mice). **E**. Analysis of segmental stiffness of carotid artery (n=10; * $P < 0.05$ *vs.* WT/Veh; $^{\#}$ $P < 0.05$ *vs.* WT/Nic mice). **F**. Representative images of M-mode for abdominal aorta monitored by ultrasound from WT and *Sirt1*^{Super} mice treated with/without nicotine. **G**. Circumferential cyclic strain of abdominal aorta in WT and *Sirt1*^{Super} mice with/without nicotine treatment (n=10; * $P < 0.05$ *vs.* WT/Veh; $^{\#}$ $P < 0.05$ *vs.* WT/Nic mice). **H**. Analysis of segmental stiffness of abdominal aorta (n=10; * $P < 0.05$ *vs.* WT/Veh; # $P < 0.05$ *vs.* WT/Nic mice). Veh, vehicle; Nic, nicotine.

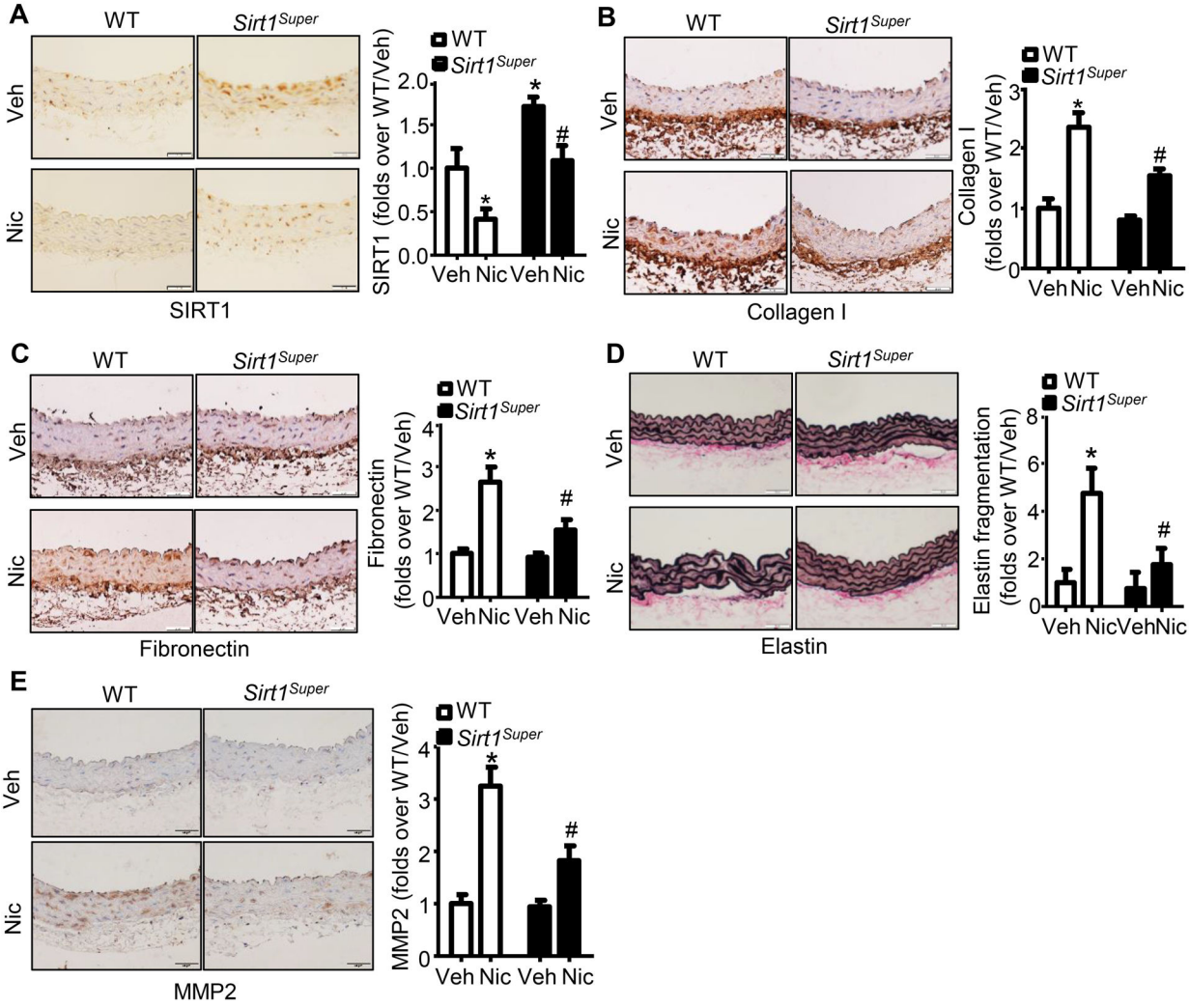

Figure 4. *Sirt1* overexpression inhibits nicotine-induced arterial extracellular matrix remodeling.

A. Representative images of IHC staining and quantification of SIRT1 in aorta from WT and *Sirt1*- overexpressing (*Sirt1*^{Super}) mice with or without nicotine treatment (n=5; * $P < 0.05$ *vs.* WT/Veh; # $P < 0.05$ *vs.* WT/Nic mice). **B**. Representative images of IHC staining and quantification of collagen I in aorta from WT and *Sirt1*^{Super} mice with or without nicotine treatment (n=5; * $P < 0.05$ *vs.* WT/Veh; # $P < 0.05$ *vs.* WT/Nic mice). **C**. Representative images of IHC staining and quantification of fibronectin in aorta from WT and *Sirt1*^{Super} mice with or without nicotine treatment (n=5; * $P < 0.05$ *vs.* WT/Veh; # $P < 0.05$ *vs.* WT/Nic mice). **D**. Representative images of Van Gieson's staining and quantification of elastin fragmentation in aorta from WT and *Sirt1*^{Super} mice with or without nicotine treatment (n=5; * $P < 0.05$ *vs.* WT/Veh; # $P < 0.05$ *vs.* WT/Nic mice). **E**. Representative images of IHC staining and quantification of MMP2 in aorta from WT and *Sirt1*^{Super} mice with or without nicotine treatment (n=5; * $P < 0.05$ *vs.* WT/Veh; # $P < 0.05$ *vs.* WT/Nic mice). Veh, vehicle; Nic, nicotine. Negative controls for staining of anti-SIRT1, anti-Collagen I, anti-Fibronectin, and anti-MMP2 were presented in Online Figure III.

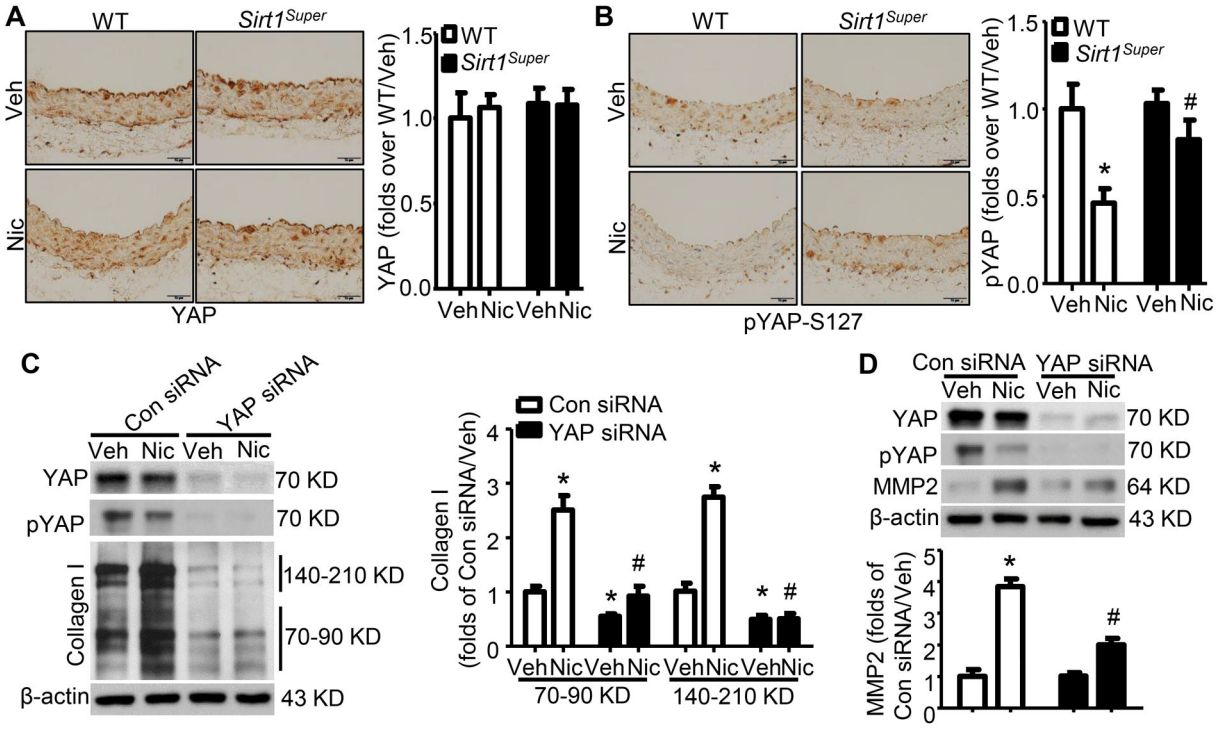

Figure 5. *Sirt1* overexpression prevents nicotine-induced YAP dephosphorylation that mediates arterial extracellular matrix remodeling.

A. Representative images of IHC staining (left panel) and quantification of YAP (right panel) in aorta from WT and *Sirt1*-overexpressing (*Sirt1*^{Super}) mice with or without nicotine treatment (n=5). **B**. Representative images of IHC staining (left panel) and quantification of pYAP (right panel) in aorta from WT and *Sirt1*^{Super} mice with or without nicotine treatment (n=5; * $P < 0.01$ *vs.* WT/Veh; $^{\#}$ $P < 0.05$ *vs.* WT/Nic mice). **C**. YAP knockdown reduced collagen I protein expression (precursor: 140–210KD; mature: 70–90KD) under vehicle and nicotine-treated condition (n=5; * $P < 0.01$ *vs.* Con siRNA/Veh; $^{\#}$ $P < 0.05$ *vs.* Con siRNA/Nic). **D**. YAP knockdown repressed nicotine-elevated MMP2 protein (n=5; * $P < 0.01$ *vs.* Con siRNA/Veh; $^{\#}$ $P < 0.05$ *vs.* Con siRNA/Nic). Veh, vehicle; Nic, nicotine. Negative controls for staining of anti-YAP and anti-pYAP-S127 were presented in Online Figure IV.

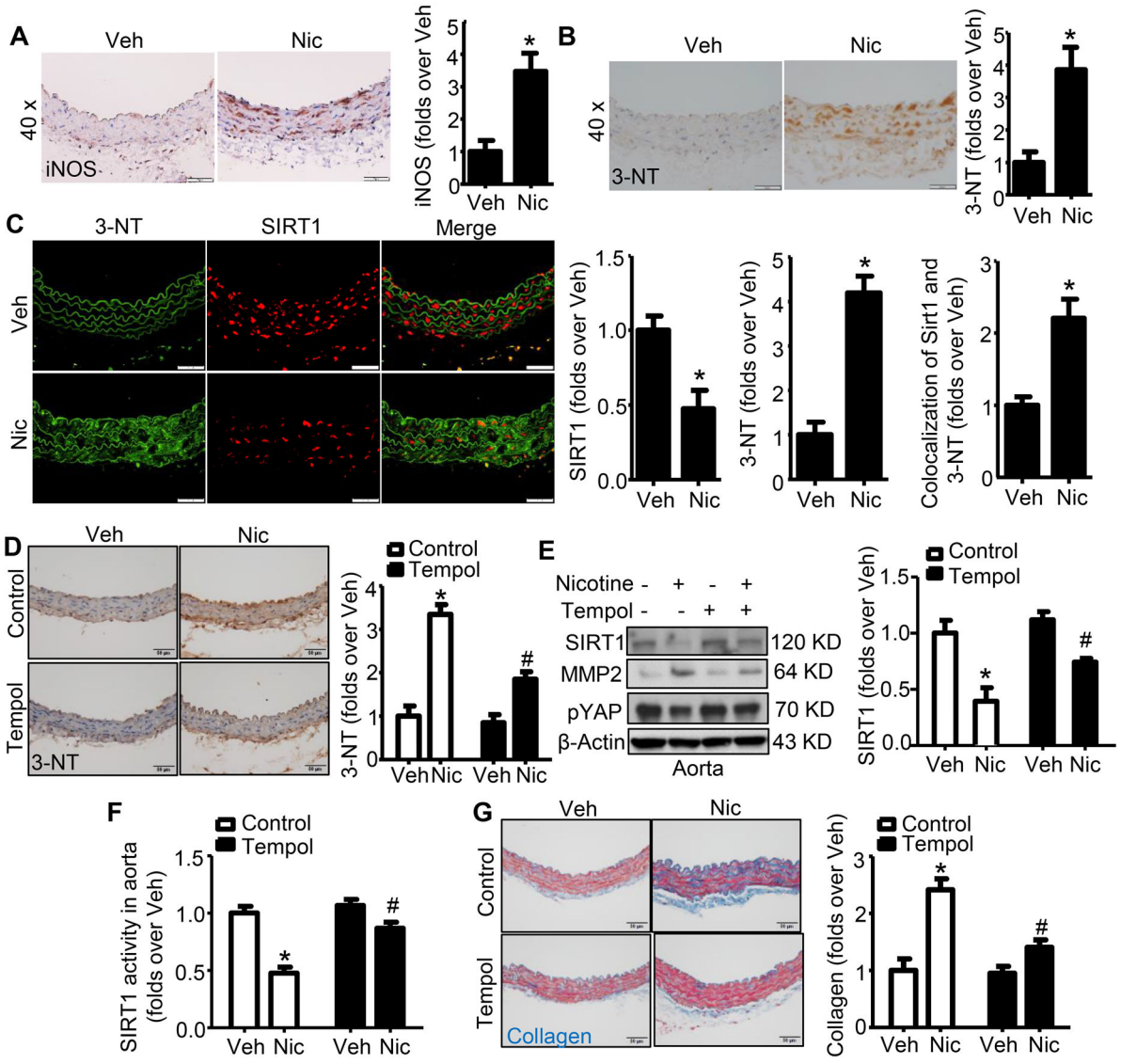

Figure 6. Nicotine upregulates peroxynitrite formation in mouse aorta *in vivo*.

A. Representative images of IHC staining and quantification of iNOS in aortas from mice with or without nicotine treatment (n=5; * $P < 0.01$ *vs.* Veh). **B**. Representative images of IHC staining and quantification of 3-nitrotyrosine (3-NT) in aortas from mice with or without nicotine treatment (n=10; * $P < 0.01$ *vs.* Veh). **C**. Representative images of immunofluoresence co-staining and quantification of 3-NT and SIRT1 in aorta from mice with or without nicotine treatment (n=10; * $P < 0.05$ *vs.* Veh). **D**. Representative images of IHC staining and quantification of 3-NT in aortas from mice with or without nicotine treatment along with control or Tempol treatment (n=5; * $P < 0.01$ *vs.* Veh; $^{\#}$ $P < 0.01$ *vs.* Nic alone). **E**. Tempol reversed nicotine-induced SIRT1 and pYAP reduction in aortas (n=5; * $P < 0.01$ *vs.* Veh; $^{\#}$ $P < 0.05$ *vs.* Nic alone). **F**. Tempol attenuated SIRT1 activity inhibition by nicotine (n=5; * $P < 0.01$ *vs.* Veh; $^{\#}$ $P < 0.05$ *vs.* Nic alone). **G**. Representative images and quantification of collagen content in aortas based on Masson trichrome staining (Blue color) of mice with/without nicotine treatment along with control or Tempol treatment (n=5;

* $P < 0.01$ *vs.* Veh; # $P < 0.01$ *vs.* Nic alone). Veh, vehicle; Nic, nicotine. Negative controls for staining of anti-iNOS and anti-3-NT were presented in Online Figure V.

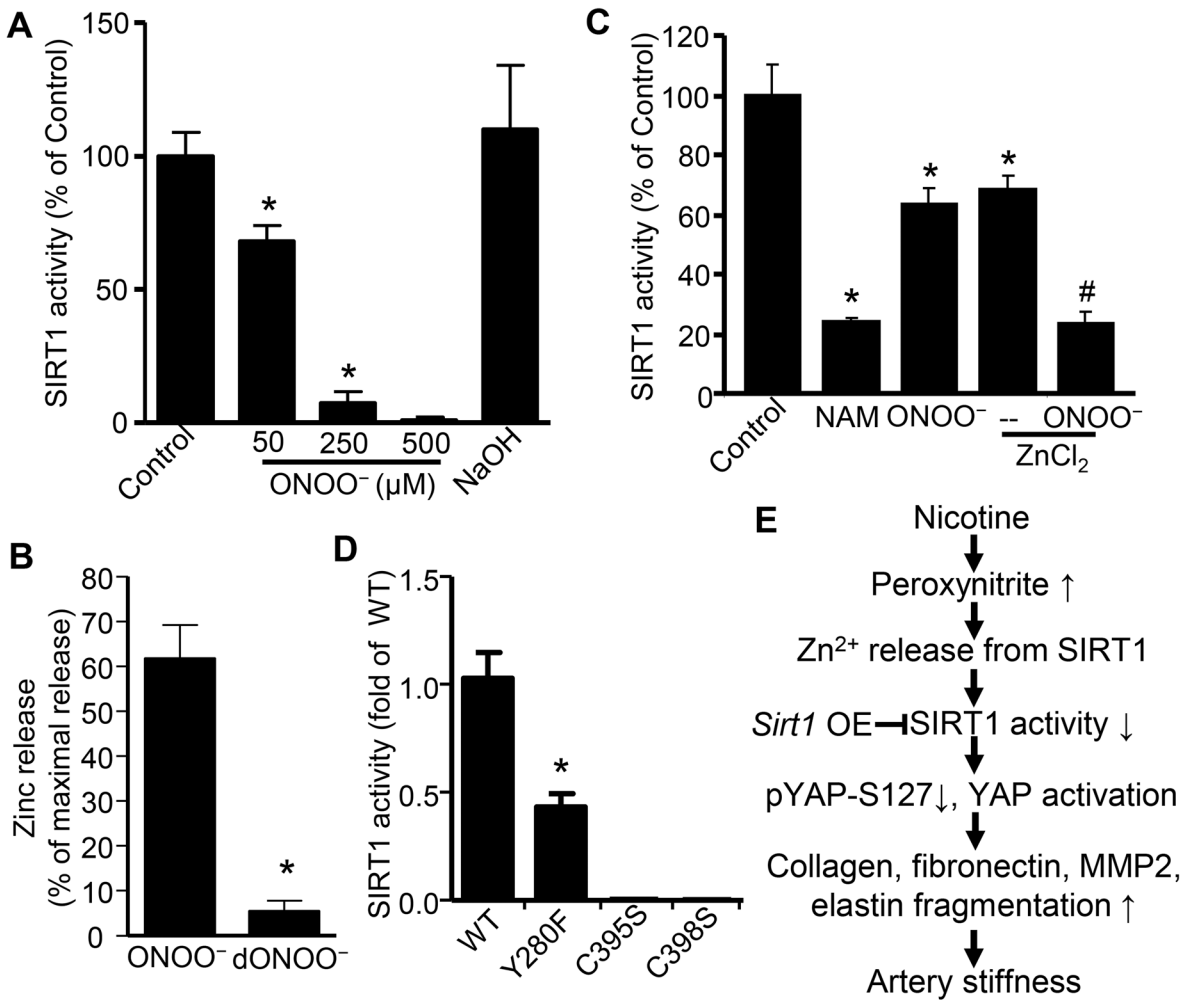

Figure 7. Peroxynitrite mediates SIRT1 inhibition and zinc release from SIRT1.

A. SIRT1 inhibition by peroxynitrite ($ONOO^-$). Human recombinant SIRT1 was treated with $ONOO^-$ in reaction system for 45 min at 37°C (n=3–6; * $P<0.001$ *vs.* control). **B**. Zinc release from recombinant human SIRT1 with indicated treatments, $ONOO^-$ (50 μM) and decomposed $ONOO^-$ ($dONOO^-$) (n=3; * $P<0.001$ *vs.* $ONOO^-$). Zinc was assayed as described in Methods and was expressed as percentage of maximal zinc release from SIRT1 diluted in 7 M guanidine HCl. **C**. Exogenous zinc inhibits SIRT1 activity. Human recombinant SIRT1 was treated in advance with nicotinamide (NAM, Catalog # N1788, 400x dilution) or $ONOO^-$ (50 μM) with or without $ZnCl_2$ for 15 min, then put in the reaction system for 30 min at 37°C (n=4; * $P<0.001$ *vs.* control. # $P<0.01$ *vs.* $ZnCl_2$. **D**. NAD^+-binding site or Zn^{2+}-binding module is required for basal SIRT1 activity. Recombinant SIRT1 proteins as indicated above were added in reaction system for 30 min at 37°C. Y, tyrosine; F, phenylalanine; C, cysteine; S, serine. (n=3–4; * $P<0.01$ *vs.* WT). **E**. Scheme of nicotine-induced arterial stiffness via peroxynitrite-mediated SIRT1 inhibition.